A nucleosome switch primes Hepatitis B Virus infection

Nicholas A. Prescott[1,2], Andrés Mansisidor[3]†, Yaron Bram[4]†, Abigail A. Lemmon[1,2], Christine Lim[4], Viviana I. Risca[3], Robert E. Schwartz[4,6*], Yael David[2,5,6*]

[1]Tri-Institutional PhD Program in Chemical Biology; New York, NY 10065, USA.

[2]Chemical Biology Program, Memorial Sloan Kettering Cancer Center; New York, NY 10065, USA.

[3]Laboratory of Genome Architecture and Dynamics, The Rockefeller University; New York, NY 10065, USA.

[4]Division of Gastroenterology & Hepatology, Department of Medicine, Weill Cornell Medicine; New York, NY 10065, USA.

[5]Department of Pharmacology, Weill Cornell Medicine; New York, NY 10065, USA.

[6]Department of Physiology and Biophysics, Weill Cornell Medicine; New York, NY 10065, USA.

*Corresponding authors. Email: davidshy@mskcc.org, res2025@med.cornell.edu

†These authors contributed equally to this work

Abstract: Chronic hepatitis B virus (HBV) infection is an incurable global health threat responsible for causing liver disease and hepatocellular carcinoma. During the genesis of infection, HBV establishes an independent minichromosome consisting of the viral covalently closed circular DNA (cccDNA) genome and host histones. The first viral protein expressed, HBx, induces degradation of a host silencing factor to facilitate infection. However, the relationship between cccDNA chromatin and early HBx transcription remains poorly understood. Establishing reconstituted viral minichromosomes, we found that nucleosomes in cccDNA drive HBx transcription. We corroborated these findings in cells and further showed that the chromatin destabilizing drug CBL137 inhibits infection in hepatocytes. Our results shed new light on a long-standing paradox and represent a novel therapeutic avenue for the treatment of chronic HBV.

One-Sentence Summary: Chromatin assembly on the Hepatitis B Virus genome drives transcription of the critical viral oncogene HBx, and thus infection.

Main Text: Over a quarter of a billion people worldwide are chronically infected by Hepatitis B Virus (HBV), leading to almost one million deaths annually despite the existence of an effective vaccine (*1*). Chronic infection with this incurable virus leaves patients at risk for advanced liver disease, including fibrosis, cirrhosis, and liver cancer (*2*). HBV is estimated to be responsible for over half of all cases of hepatocellular carcinoma (*3*). After viral entry into hepatocytes via the sodium taurocholate co-transporting polypeptide bile acid receptor (NTCP), the 3.2 kb HBV genome is shuttled into the nucleus and repaired from a partially double-stranded, relaxed circular DNA (rcDNA) species into fully double-stranded, covalently closed circular DNA (cccDNA) by host cell lagging strand synthesis machinery (*4–6*). The cccDNA rapidly becomes populated with host histone octamers and serves as the primary template for viral transcription (*7–9*). This viral minichromosome establishes a distinct chromatin state and is decorated predominantly with active transcription-associated histone post-translational modifications (PTMs) (*7*, *10*, *11*). Although the precise details of this process are not fully resolved, so-called "epigenetic" drugs targeting chromatin-modifying factors have emerged as attractive potential therapeutic opportunities in HBV (*12*, *13*). Presently, long-term treatment with oral nucleos(t)ide analogs or short-term treatment with interferon-alpha injections remains the standard of care to halt viral proliferation, but these fall short of eradicating cccDNA in infected hepatocytes (*2*). The current inability to therapeutically target cccDNA allows the minichromosome to persist and sustain chronic infection.

Even in cases with long-term antiviral treatment, basal levels of the HBV-encoded oncoprotein HBx remain in hepatocytes and can promote disease progression (*1*, *14*). Intriguingly, HBx has a paradoxical relationship to cccDNA transcription during the earliest stages of infection (*12*). HBx induces the degradation of the host Smc5/6 complex, which otherwise would transcriptionally silence cccDNA, but it is absent from the mature virion and must be expressed *de novo* in freshly infected hepatocytes (*15*, *16*). HBx is thought to be the earliest-expressed viral gene, with its transcript most abundant in the first 24 hours after HBV infection (*17*, *18*). Although some reports have identified HBx mRNA circulating in the supernatant of infected cells and in plasma of infected patients, it has yet to be proven if it is packaged alongside HBV rcDNA in virions (*17*, *19*). Additionally, the interplay between cccDNA chromatin state and viral transcription kinetics remains poorly understood despite its potential importance in the establishment of active chronic infection. Traditional genetic and cell biology approaches lack the temporal and biochemical resolution necessary to characterize this critical intermediate in HBV infection establishment. To surmount these difficulties, we developed a method to generate recombinant cccDNA minichromosomes in a chemically defined system, allowing us to characterize its biophysical properties and map nucleosome occupancy on the chromosome. These reveal a -1/+1 nucleosomal positioning signature at the HBx transcription start site. We apply biochemical techniques to demonstrate that chromatin assembly on cccDNA is critical for expression of the HBx mRNA, but not other viral transcripts. Finally, we demonstrate that small molecule-mediated disruption of nucleosome integrity on cccDNA is sufficient to inhibit HBx transcription and viral infection in hepatocytes.

Generation and validation of recombinant cccDNA minichromosomes

Previous approaches to generate recombinant cccDNA have largely relied on recombination-based methods, which leave undesirable exogenous DNA "scars" in the viral genome, or laborious multi-step preparations of rcDNA for repair by recombinant proteins with comparatively low yields (*5*, *20*, *21*). Moreover, the only reports of reconstituted viral

minichromosomes used *Xenopus* nuclear extracts, resulting in chemically heterogeneous products unsuitable for detailed biochemical interrogation (*9*). To overcome these limitations, we generated scarless recombinant cccDNA via enzymatic ligation of purified double-stranded linear HBV DNA (dslDNA), as has been done previously to generate DNA minicircles for studies of chromatin topology (Fig. 1A, Fig. S1A) (*22*). To validate the infectious capacity of recombinant cccDNA, we transfected HepG2 cells with cccDNA and assayed for hallmarks of HBV infection. Intracellular viral RNA and secreted viral DNA were readily detected for up to two weeks post-transfection (Fig. 1B). Likewise, HBV surface antigen and secreted antigens (HBsAg and HBeAg, respectively) were abundant in the supernatant of transfected cells (Fig. S1B). Finally, virions collected from the supernatant of cccDNA-transfected cells proved capable of inducing infection when added to HepG2-NTCP cells, which were then subject to immunofluorescence to detect intracellular viral capsid protein (HBcAg) (Fig S1C). Together, these results validate our construct as a physiologically relevant tool to establish and study *bona fide* HBV infections.

We next tested our recombinant cccDNA as a substrate for *in vitro* chromatin assembly to produce recombinant viral minichromosomes. To do so, we combined recombinant canonical human histone octamers with the synthetic viral DNA and performed chromatin assembly via salt gradient dialysis. Histone incorporation into both dslDNA and cccDNA was first validated by electrophoretic mobility shift assay of the intact chromatin fibers (Fig. 1C). We subsequently visualized empty and chromatinized cccDNA with atomic force microscopy (AFM). The collected micrographs illustrate the robust assembly of recombinant histone octamers and cccDNA into minichromosomes (Fig 1D). We next sought to compare the basic biophysical characteristics of HBV minichromosomes and similarly sized nucleosome arrays often used to mimic eukaryotic chromatin. We thus generated corresponding linear and circular constructs containing 18 repeats of the Widom 601 strong nucleosome positioning sequence with 30 bp of linker DNA ($Lin601^{18}$ and $Cir601^{18}$, respectively), matching both the length and predicted number of nucleosomes in the HBV genome, and assembled them into chromatin fibers (Fig. S2A-C) (*23*, *24*). We next quantitated a basal compaction metric for nucleosome arrays of all four species by measuring the ratio between the volume and the surface area of individual particles in AFM micrographs (Fig. S2D). To orthogonally compare compaction, we also measured the readiness of nucleosome arrays to precipitate in a magnesium-dependent self-association assay (Fig. S2E) (*25*). HBV chromatin arrays displayed similar compaction scores as measured by AFM and rates of precipitation in the self-association assays as the 601 arrays, suggesting comparable biophysical properties. Finally, we sought to determine whether the reconstituted viral chromatin displayed a DNA-intrinsic nucleosome organization or stochastic positioning of histone octamers. Micrococcal nuclease digestion followed by sequencing (MNase-seq) of both cccDNA and dslDNA chromatin arrays revealed a conserved chromatin architecture between the two species, suggesting a high degree of sequence-intrinsic nucleosome positioning by the HBV genome seemingly unaffected by template circularization or possible torsional strain (Fig. 1E, S2F). Both species displayed a collection of tightly positioned nucleosome core particles, as well as some poorly phased nucleosomes with potentially more stochastic positioning. Altogether, the results of these experiments validate our reconstitution of cccDNA minichromosomes and open the door to further investigation with them.

Chromatin occupancy of reconstituted cccDNA impacts viral transcription

To understand the role of chromatin in HBV transcription during early infection, we first tested the capacity of the recombinant cccDNA to serve as a template for *in vitro* transcription.

Specifically, we incubated both empty and chromatinized cccDNA with human nuclear extract and used RT-qPCR assay to quantify total viral RNA after one hour. Unexpectedly, we detected a significant increase in the total transcriptional output of the chromatinized template compared to empty DNA (Fig. 2A). These results seemed counterintuitive, as conventionally nucleosomes are considered obstacles for RNA Polymerase II to traverse rather than facilitators of gene expression (*26*, *27*). On the contrary, our results suggest that chromatin enhances transcription from cccDNA. To further investigate this possibility, we generated a series of cccDNA minichromosomes with increasing levels of histone saturation for use as *in vitro* transcription templates – undersaturated, intermediately saturated, or fully saturated – by altering the stoichiometry of histone octamer to DNA during chromatin assembly. The different chromatin species were qualitatively distinct from one another when visualized by AFM (Fig. 2B). Additionally, as predicted, increasing histone octamer saturation correlated with greater chromatin compaction (Fig. 2C).

In order to monitor specific viral transcripts, rather than global HBV transcription more generally, we also turned to a more specific RT-qPCR assay to enable quantitation of the four major viral transcripts – the 3.5 kb preC transcript (also called the pregenomic RNA, encoding both HBcAg and the viral polymerase), the 2.4 kb preS1 transcript (encoding the longest HBsAg isoform), the 2.1 kb preS2 transcript (encoding two shorter HBsAg isoforms), and the 0.7-0.9 kb X transcript (encoding HBx) (*28*). Applying this assay to measure the transcriptional output of our differentially saturated cccDNA minichromosomes revealed that indeed, not all viral transcripts respond equally to the presence of chromatin (Fig. 2D). While the preS1 and preS2 transcripts exhibit no significant changes in expression upon template chromatinization, the preC transcript displayed significantly increased transcription upon template chromatinization although it was still expressed from empty DNA. Of note, there was no significant difference between the output of templates from the three different saturation levels. Strikingly, we observed a switch-like behavior for the X transcript: empty and undersaturated cccDNA did not produce any detectable X transcript, whereas the two highest saturation templates produced it abundantly. The notion that a critical early gene in viral infection could exhibit a requirement for nucleosome occupancy motivated us to further explore the relationship between chromatin organization and HBx transcription.

Early HBx expression is linked to the cccDNA nucleosome landscape

To first assess the chromatin landscape of cccDNA, we consulted published datasets. Across HBV-infected HepG2-NTCP cells, primary human hepatocytes, and patient liver samples, chromatin-immunoprecipitation followed by sequencing (ChIP-seq) data show strong signal for the transcription start site (TSS)-associated histone PTM H3K4me3 and RNA Polymerase II across the viral genome. Interestingly, these signals closely matched bulk nucleosome occupancy across the samples as well (Fig. 3A, Fig. S3) (*11*). To test if our differentially saturated *in vitro* chromatin species reflected similar nucleosome occupancy patterns as the published datasets, we next performed a similar MNase-seq experiment. All three chromatinized samples yielded peaks of mononucleosome-sized DNA fragment coverage at similar loci across the viral genome, though the signal strength for certain peaks varied between samples (Fig. 3B, Fig. S4). For example, the strongest nucleosome occupancy signal across all three samples was centered around nt 1269 at the 3' end of the HBx open reading frame (ORF) and just upstream of the preC/pgRNA TSS. In contrast, the two samples with the highest saturation state, which were able to produce X transcript *in vitro* (intermediately and fully saturated), displayed stronger peaks around the putative HBx TSS compared to the under-

saturated sample. This result suggests the presence of more strongly-positioned -1 and +1 nucleosomes around this site in the increasingly saturated samples, as observed at active TSSs throughout eukaryotic genomes (*29*, *30*). Gratifyingly, the regions around the -1 and +1 nucleosomes we identified at the X TSS are also enriched with H3K4me3 in the published datasets, corroborating our theory that the X TSS is flanked by these features *in vivo* (Fig. 3A). Although our MNase-seq results did not precisely match the nucleosome occupancy from published datasets, we speculated this could potentially be due to changes in chromatin dynamics of cccDNA based on the time since infection. Since all available datasets are from cells at minimum one-week post-infection, we set out to determine cccDNA nucleosome occupancy during early timepoints of infection. To avoid the temporal heterogeneity and sample abundance limitations of traditional cellular infection models, we transfected empty recombinant cccDNA into HEK293T cells. Cells were then subjected to MNase-seq after 4 or 24 hours. At both timepoints, nucleosome-sized fragment coverage (~120-200 bp) was detectable across most of the viral genome (Fig. 3C, Fig. S5). We observed fewer well-defined nucleosomes in the transfected cells than in the reconstituted viral chromosomes, with the signal for both timepoints appearing similar to the published ChIP-seq data. However, two regions of the HBV genome were relatively unoccupied by nucleosomes, corresponding to putative TSSs for the preS1 and X transcripts, suggesting a classical nucleosome-depleted region flanked by -1 and +1 nucleosomes.

Having surveyed the nucleosome organization of cccDNA, we also sought to assess the kinetics of HBV transcription during the earliest stages of infection. To do so, we transfected HEK293T cells with recombinant cccDNA and sequenced poly(A)-enriched RNA 4- and 24-hours post-transfection (Fig. 3D). Concordant with literature precedent for HBV infection, modest human gene expression changes were detected in transfected cells compared to non-transfected cells at any timepoint (Fig. S6). At all timepoints post-transfection, sequencing reads readily aligned to both the HBV and human genomes (Fig. 3E). By 12 hours, sequencing reads mapping across the entire HBV genome rendered us unable to discern specific transcript species due to their overlapping nature. However, at the earliest timepoints (4 and 8 hours) RNA-seq reads formed a peak centered around the HBx ORF, suggesting that X is the first viral transcript to accumulate in newly infected cells (Fig. 3D). Quantification of the fraction of HBV reads mapping to the HBx ORF, which comprises only 28 % of the viral genome, indeed showed that at the earliest timepoints upwards of 60 % of sequencing reads map to HBx (Fig. 3E). Together these data suggest a strong correlation between early HBV chromatinization and HBx transcription, with both being critical steps during the first hours of infection.

Nucleosome destabilizing drugs disrupt cccDNA integrity *in vitro* and inhibit viral transcription in cells

Based on our results suggesting that chromatinization of cccDNA is necessary for HBx transcription, we hypothesized that disruption of chromatin assembly would affect viral infection. Nucleosome assembly in cells relies on an intricate network of histone variants and chaperones, ATP-dependent chromatin remodelers, replisome components, and other structural proteins within the nucleus (*31*). Relatively few pharmacological options are available to specifically inhibit chromatin assembly factors, but we acquired and tested five small molecule inhibitors of histone chaperones, chromatin remodelers, or replication factors: the BAF complex inhibitors PFI-3 and BD98, the indirect FACT complex inhibitor CBL137, and the Cdc7 kinase inhibitors TAK-931 and PHA-767491, as Cdc7 kinase activity has been shown to activate the H3-H4 chaperone CAF-1 (*32–37*). Following a 24-hour pre-treatment with each inhibitor, HEK

293T cells were transfected with recombinant cccDNA and continued drug treatment until harvesting 4, 8, or 24 hours later for analysis. None of the doses used impacted cell viability for up to 48 hours of treatment, and while four of the molecules tested showed no consistent effect, CBL137 was able to significantly inhibit viral transcription at all three timepoints (Fig. 4A, Fig. S7). This effect proved to be dose-dependent, with CBL137 displaying an EC_{50} of approximately 135 nM in cells transfected with cccDNA and treated with the drug concurrently for 24 hours (Fig. 4B).

CBL137 was first described as an inhibitor of the histone H2A-H2B chaperone FACT complex, capable of redistributing it in nuclei to activate p53 and suppress NF-kB (*34*). More recently the mechanism of FACT inhibition by CBL137 has been elucidated, and CBL137 was shown to intercalate into nucleosomal DNA, disrupting nucleosome integrity and trapping FACT on destabilized chromatin, which prevents it from chaperoning H2A-H2B dimers elsewhere across the genome (e.g., at transcription sites) (*38*). This motivated us to test if the anti-HBV effect of CBL137 is due to chromatin destabilization, rather than formal inhibition of FACT. To do so, we first tested the ability of CBL137 and other molecules previously shown to induce histone eviction from chromatin (the anthracycline topoisomerase II inhibitors aclarubicin and doxorubicin) to destabilize recombinant mononucleosomes *in vitro* (*39*). Indeed, as evidenced by an increase in free DNA and precipitated chromatin in the native nucleosome EMSA gel, CBL137, doxorubicin, and aclarubicin destabilized nucleosome core particles, whereas the chemically distinct topoisomerase II inhibitor etoposide and the DNA-binding dye Hoechst did not (Fig. 4C) Importantly, we found that CBL137, aclarubicin, and doxorubicin were similarly able to induce a marked destabilization of intact reconstituted HBV chromatin arrays, with drug treatment causing chromatin fibers to oligomerize and run as a smear rather than a clear band on a native gel (Fig. 4D). Based on these results, we sought to determine whether anthracycline treatment on cells would have a similar effect on HBx transcription as CBL137 treatment, focusing on the molecule aclarubicin rather than doxorubicin to avoid any potential confounding effects from doxorubicin-induced DNA damage (*39*). Indeed, aclarubicin treatment was able to diminish HBV transcription in cells transfected with recombinant cccDNA (Fig. 4E).

CBL137 inhibits viral transcription, antigen secretion, and genome replication in hepatocyte models of HBV infection

With the inhibition of chromatin stability posing a potential therapeutic opportunity for HBV, we chose to continue studies with CBL137 directly in hepatocytes, the target tissue of the virus. We performed similar experiments transfecting recombinant cccDNA into HepG2 cells. As expected, total viral RNA was significantly reduced in CBL137-treated cells at 4-hours after transfection, and almost completely abolished by 24-hours (Fig. 5A). To confirm this observation in other cellular models of HBV infection, we turned to HepG2.2.15 cells, which contain chromosomally integrated copies of the HBV genome (*40*). We found that long-term growth of cells in media containing a low dose of 50 nM CBL137 produced a consistent reduction in total HBV RNA within 3 days and up to 11 days of culture without harming cell viability (Fig. 5B, S7H). Encouraged by our results with CBL137 on simpler HBV model systems, we sought to characterize its potential as a treatment option using a *bona fide* infection model. To do so we cultured HepG2-NTCP cells and infected them with HBV, while also treating with 125 nM CBL137 either one day prior to infection and/or one day following infection. Six days after infection, media was collected from each sample and subjected to ELISA measurements for the secreted viral antigens HBeAg and HBsAg (Fig. 5C). Both post-infection and combined pre- and post-infection treatments led to significant reduction in viral antigen secretion, while the pre-

treatment only yielded negligible changes compared to DMSO treated cells. In addition to viral protein secretion, we also investigated whether CBL137 treatment either pre- or post-infection could reduce viral genome replication (Fig. 5D). Indeed, even 1 day pre-treatment of cells with the drug was able to significantly diminish both secreted rcDNA titer in media and intracellular cccDNA levels to approximately 25 % of those in untreated cells. Even more strikingly, post-infection treatment for 5 days led to near total elimination of secreted rcDNA from media and reduced cccDNA levels to only 5 % of untreated cells. Together, these results suggest that treatment with CBL137 can not only hamper viral transcription during early stages of infection, but also reduce viral protein secretion and genome replication in hepatocytes.

Discussion

Here, we report the first robust platform to generate reconstituted HBV minichromosomes, laying the foundation for mechanistic investigations of a critical species in viral pathogenesis. This recombinant, functional cccDNA serves as a powerful tool to surmount the temporal heterogeneity and abundance limitations of viral infection, enabling closer study of early infection timepoints. We utilized this system to perform biochemical investigations that led to a model wherein chromatin occupancy on cccDNA, particularly the establishment of -1 and +1 nucleosomes around the HBx TSS, plays a pivotal role in its transcription and thus HBV infection (Fig. 5D). We corroborated our *in vitro* results with a suite of transcriptomic, nucleosome mapping, and pharmacological experiments, and have shown that this phenomenon may have important clinical implications as a therapeutic or prophylactic treatment for chronic HBV infection in the future.

The results of our work also contribute insights into ongoing discussions about the basic biology of HBV infection. The rapid kinetics of HBx expression seen in our RNA-seq data (Fig. 3D, E) compared to other viral transcripts is consistent with previous studies of HBV transcript kinetics, as well as the intuitive notion that for infection to progress, HBx must appear rapidly in order to induce the degradation of Smc5/6 that would otherwise suppress infection (*15*, *16*, *18*). Several reports have found HBx RNAs in viral particles circulating in patient sera samples and in the supernatant of infected cell lines, leading to an outstanding question in the field - whether HBx mRNA needs to be delivered to naïve hepatocytes alongside rcDNA (*17*, *19*, *41*). Our data show that introduction of cccDNA to wild-type cells is sufficient for HBx expression. How HBx can be so rapidly and specifically expressed without Smc5/6-induced viral silencing remains a topic for future studies.

The mechanism by which the presence of -1 and +1 nucleosomes around the HBx TSS might facilitate this specific gene's transcription merits deeper investigation. Luciferase-based reporter assays have previously shown that the HBx promoter is comparatively weaker than those of other HBV transcripts – a finding also supported by the weaker signal for the X transcript in Northern blot assays (*11*, *42*). One possible explanation to reconcile these findings may arise from recent structural and biochemical studies showing that PIC-Mediator, the mega-complex responsible for eukaryotic transcription initiation, binds to the +1 nucleosome and can enhance transcription for TATA-like and TATA-less promoters (*43*). No TATA or TATA-like element has been identified for HBx, although such elements have been described elsewhere in the HBV genome (*44*). Thus, an attractive hypothesis is that nucleosome assembly at the HBx TSS drives transcription by allowing PIC-Mediator to recognize a gene which otherwise cannot recruit the basal transcription machinery based on DNA sequence alone.

Our results indicating that pharmacological perturbation of chromatin integrity hampers HBV infection provide a new potential therapeutic avenue while also underscoring the need to characterize the epigenetic landscape of cccDNA more robustly. Although such efforts have been undertaken in duck HBV (*23*), we describe some of the first high-resolution characterization of nucleosome positioning across the HBV genome in mammalian cells (Fig. 3C). Similarly sparse is our knowledge of histone modifications and variants in cccDNA. Other studies have found that cccDNA is decorated overwhelmingly with active transcription-associated PTMs, and mapped positions of H3K4me3, H3K27ac, and H3K122ac, among others, along the genome (*11*, *45*). Lower resolution methods have also been applied to identify other PTMs, such as H4ac, and more recently the histone variant H3.3 on cccDNA (*10*, *46*, *47*). As more is known about the chromatin of cccDNA, therapeutic opportunities may become available to target the minichromosome if not for degradation, then to silence it and establish a functional cure (*48*). Finally, our promising results for chromatin destabilization as a means to target HBV infection leave the door open to investigate similar approaches on other chromatinized DNA viruses including herpesviruses, papillomaviruses, and adenoviruses.

References

1. M.-F. Yuen, D.-S. Chen, G. M. Dusheiko, H. L. A. Janssen, D. T. Y. Lau, S. A. Locarnini, M. G. Peters, C.-L. Lai, Hepatitis B virus infection. *Nat. Rev. Dis. Primer*. **4**, 18035 (2018).

2. W.-K. Seto, Y.-R. Lo, J.-M. Pawlotsky, M.-F. Yuen, Chronic hepatitis B virus infection. *The Lancet*. **392**, 2313–2324 (2018).

3. M. Levrero, J. Zucman-Rossi, Mechanisms of HBV-induced hepatocellular carcinoma. *J. Hepatol.* **64**, S84–S101 (2016).

4. H. Yan, G. Zhong, G. Xu, W. He, Z. Jing, Z. Gao, Y. Huang, Y. Qi, B. Peng, H. Wang, L. Fu, M. Song, P. Chen, W. Gao, B. Ren, Y. Sun, T. Cai, X. Feng, J. Sui, W. Li, Sodium taurocholate cotransporting polypeptide is a functional receptor for human hepatitis B and D virus. *eLife*. **2012**, 1–28 (2012).

5. L. Wei, A. Ploss, Core components of DNA lagging strand synthesis machinery are essential for hepatitis B virus cccDNA formation. *Nat. Microbiol.* **5**, 715–726 (2020).

6. L. Wei, A. Ploss, Hepatitis B virus cccDNA is formed through distinct repair processes of each strand. *Nat. Commun.* **12**, 1591 (2021).

7. T. Pollicino, L. Belloni, G. Raffa, N. Pediconi, G. Squadrito, G. Raimondo, M. Levrero, Hepatitis B Virus Replication Is Regulated by the Acetylation Status of Hepatitis B Virus cccDNA-Bound H3 and H4 Histones. *Gastroenterology*. **130**, 823–837 (2006).

8. C.-T. Bock, P. Schranz, C. H. Schröder, H. Zentgraf, Hepatitis B virus genome is organized into nucleosomes in the nucleus of the infected cell. *Virus Genes*. **8**, 215–229 (1994).

9. C. T. Bock, S. Schwinn, S. Locarnini, J. Fyfe, M. P. Manns, C. Trautwein, H. Zentgraf, Structural organization of the hepatitis B virus minichromosome. *J. Mol. Biol.* **307**, 183–196 (2001).

10. L. Belloni, T. Pollicino, F. De Nicola, F. Guerrieri, G. Raffa, M. Fanciulli, G. Raimondo, M. Levrero, Nuclear HBx binds the HBV minichromosome and modifies the epigenetic regulation of cccDNA function. *Proc. Natl. Acad. Sci.* **106**, 19975–19979 (2009).

11. P. Tropberger, A. Mercier, M. Robinson, W. Zhong, D. E. Ganem, M. Holdorf, Mapping of histone modifications in episomal HBV cccDNA uncovers an unusual chromatin organization amenable to epigenetic manipulation. *Proc. Natl. Acad. Sci.* **112**, E5715–E5724 (2015).

12. N. A. Prescott, Y. Bram, R. E. Schwartz, Y. David, Targeting Hepatitis B Virus Covalently Closed Circular DNA and Hepatitis B Virus X Protein: Recent Advances and New Approaches. *ACS Infect. Dis.* **5**, 1657–1667 (2019).

13. L. Yang, T. Zou, Y. Chen, Y. Zhao, X. Wu, M. Li, F. Du, Y. Chen, Z. Xiao, J. Shen, Hepatitis B virus X protein mediated epigenetic alterations in the pathogenesis of hepatocellular carcinoma. *Hepatol. Int.* **16**, 741–754 (2022).

14. B. L. Slagle, M. J. Bouchard, Role of HBx in hepatitis B virus persistence and its therapeutic implications. *Curr. Opin. Virol.* **30**, 32–38 (2018).

15. A. Decorsière, H. Mueller, P. C. van Breugel, F. Abdul, L. Gerossier, R. K. Beran, C. M. Livingston, C. Niu, S. P. Fletcher, O. Hantz, M. Strubin, Hepatitis B virus X protein identifies the Smc5/6 complex as a host restriction factor. *Nature*. **531**, 386–380 (2016).

16. C. M. Murphy, Y. Xu, F. Li, K. Nio, N. Reszka-Blanco, X. Li, Y. Wu, Y. Yu, Y. Xiong, L. Su, Hepatitis B Virus X Protein Promotes Degradation of SMC5/6 to Enhance HBV Replication. *Cell Rep.* **16**, 2846–2854 (2016).

17. C. Niu, C. M. Livingston, L. Li, R. K. Beran, S. Daffis, D. Ramakrishnan, D. Burdette, L. Peiser, E. Salas, H. Ramos, M. Yu, G. Cheng, M. Strubin, W. E. Delaney IV, S. P. Fletcher, The Smc5/6 Complex Restricts HBV when Localized to ND10 without Inducing an Innate Immune Response and Is Counteracted by the HBV X Protein Shortly after Infection. *PLOS ONE*. **12**, e0169648 (2017).

18. H.-L. Wu, P.-J. Chen, M.-H. Lin, D.-S. Chen, Temporal aspects of major viral transcript expression in hep G2 cells transfected with cloned hepatitis B virus DNA: With emphasis on the X transcript. *Virology*. **185**, 644–651 (1991).

19. B. Stadelmayer, A. Diederichs, F. Chapus, M. Rivoire, G. Neveu, A. Alam, L. Fraisse, K. Carter, B. Testoni, F. Zoulim, Full-length 5'RACE identifies all major HBV transcripts in HBV-infected hepatocytes and patient serum. *J. Hepatol.* **73**, 40–51 (2020).

20. Z. Yan, J. Zeng, Y. Yu, K. Xiang, H. Hu, X. Zhou, L. Gu, L. Wang, J. Zhao, J. A. T. Young, L. Gao, HBVcircle: A novel tool to investigate hepatitis B virus covalently closed circular DNA. *J. Hepatol.* **66**, 1149–1157 (2017).

21. X. Guo, P. Chen, X. Hou, W. Xu, D. Wang, T. Y. Wang, L. Zhang, G. Zheng, Z. L. Gao, C. Y. He, B. Zhou, Z. Y. Chen, The recombined cccDNA produced using minicircle

technology mimicked HBV genome in structure and function closely. *Sci. Rep.* **6**, 1–10 (2016).

22. T. Nikitina, D. Norouzi, S. A. Grigoryev, V. B. Zhurkin, DNA topology in chromatin is defined by nucleosome spacing. *Sci. Adv.* **3**, e1700957 (2017).

23. L. Shi, S. Li, F. Shen, H. Li, S. Qian, D. H. S. Lee, J. Z. Wu, W. Yang, Characterization of Nucleosome Positioning in Hepadnaviral Covalently Closed Circular DNA Minichromosomes. *J. Virol.* **86**, 10059–10069 (2012).

24. P. T. Lowary, J. Widom, New DNA sequence rules for high affinity binding to histone octamer and sequence-directed nucleosome positioning. *J. Mol. Biol.* **276**, 19–42 (1998).

25. P. M. Schwarz, A. Felthauser, T. M. Fletcher, J. C. Hansen, Reversible Oligonucleosome Self-Association: Dependence on Divalent Cations and Core Histone Tail Domains †. *Biochemistry*. **35**, 4009–4015 (1996).

26. L. Bintu, T. Ishibashi, M. Dangkulwanich, Y. Y. Wu, L. Lubkowska, M. Kashlev, C. Bustamante, Nucleosomal elements that control the topography of the barrier to transcription. *Cell*. **151**, 738–749 (2012).

27. C. M. Weber, S. Ramachandran, S. Henikoff, Nucleosomes Are Context-Specific, H2A.Z-Modulated Barriers to RNA Polymerase. *Mol. Cell*. **53**, 819–830 (2014).

28. V. D'Arienzo, A. Magri, J. M. Harris, P. A. C. Wing, C. Ko, C. O. Rubio, P. A. Revill, U. Protzer, P. Balfe, J. A. McKeating, A PCR assay to quantify patterns of HBV transcription. *J. Gen. Virol.* **102** (2021), doi:10.1099/jgv.0.001373.

29. V. Haberle, A. Stark, Eukaryotic core promoters and the functional basis of transcription initiation. *Nat. Rev. Mol. Cell Biol.* **19**, 621–637 (2018).

30. C. Jiang, B. F. Pugh, Nucleosome positioning and gene regulation: advances through genomics. *Nat. Rev. Genet.* **10**, 161–172 (2009).

31. C. M. Hammond, C. B. Strømme, H. Huang, D. J. Patel, A. Groth, Histone chaperone networks shaping chromatin function. *Nat. Rev. Mol. Cell Biol.* **18**, 141–158 (2017).

32. O. Fedorov, J. Castex, C. Tallant, D. R. Owen, S. Martin, M. Aldeghi, O. Monteiro, P. Filippakopoulos, S. Picaud, J. D. Trzupek, B. S. Gerstenberger, C. Bountra, D. Willmann, C. Wells, M. Philpott, C. Rogers, P. C. Biggin, P. E. Brennan, M. E. Bunnage, R. Schüle, T. Günther, S. Knapp, S. Müller, Selective targeting of the BRG/PB1 bromodomains impairs embryonic and trophoblast stem cell maintenance. *Sci. Adv.* **1** (2015), doi:10.1126/sciadv.1500723.

33. E. C. Dykhuizen, L. C. Carmody, N. Tolliday, G. R. Crabtree, M. A. J. Palmer, Screening for inhibitors of an essential chromatin remodeler in mouse embryonic stem cells by monitoring transcriptional regulation. *J. Biomol. Screen.* **17**, 1221–1230 (2012).

34. A. V. Gasparian, C. A. Burkhart, A. A. Purmal, L. Brodsky, M. Pal, M. Saranadasa, D. A. Bosykh, M. Commane, O. A. Guryanova, S. Pal, A. Safina, S. Sviridov, I. E. Koman, J. Veith, A. A. Komar, A. V. Gudkov, K. V. Gurova, Curaxins: Anticancer Compounds That Simultaneously Suppress NF- B and Activate p53 by Targeting FACT. *Sci. Transl. Med.* **3**, 95ra74-95ra74 (2011).

35. K. Iwai, T. Nambu, R. Dairiki, M. Ohori, J. Yu, K. Burke, M. Gotou, Y. Yamamoto, S. Ebara, S. Shibata, R. Hibino, S. Nishizawa, T. Miyazaki, M. Homma, Y. Oguro, T. Imada, N. Cho, N. Uchiyama, A. Kogame, T. Takeuchi, O. Kurasawa, K. Yamanaka, H. Niu, A. Ohashi, Molecular mechanism and potential target indication of TAK-931, a novel CDC7-selective inhibitor. *Sci. Adv.* **5**, eaav3660 (2019).

36. A. Montagnoli, B. Valsasina, V. Croci, M. Menichincheri, S. Rainoldi, V. Marchesi, M. Tibolla, P. Tenca, D. Brotherton, C. Albanese, V. Patton, R. Alzani, A. Ciavolella, F. Sola, A. Molinari, D. Volpi, N. Avanzi, F. Fiorentini, M. Cattoni, S. Healy, D. Ballinari, E. Pesenti, A. Isacchi, J. Moll, A. Bensimon, E. Vanotti, C. Santocanale, A Cdc7 kinase inhibitor restricts initiation of DNA replication and has antitumor activity. *Nat. Chem. Biol.* **4**, 357–365 (2008).

37. A. Gérard, S. Koundrioukoff, V. Ramillon, J. Sergère, N. Mailand, J. Quivy, G. Almouzni, The replication kinase Cdc7-Dbf4 promotes the interaction of the p150 subunit of chromatin assembly factor 1 with proliferating cell nuclear antigen. *EMBO Rep.* **7**, 817–823 (2006).

38. H.-W. Chang, M. E. Valieva, A. Safina, R. V. Chereji, J. Wang, O. I. Kulaeva, A. V. Morozov, M. P. Kirpichnikov, A. V. Feofanov, K. V. Gurova, V. M. Studitsky, Mechanism of FACT removal from transcribed genes by anticancer drugs curaxins. *Sci. Adv.* **4** (2018), doi:10.1126/sciadv.aav2131.

39. B. Pang, X. Qiao, L. Janssen, A. Velds, T. Groothuis, R. Kerkhoven, M. Nieuwland, H. Ovaa, S. Rottenberg, O. Van Tellingen, J. Janssen, P. Huijgens, W. Zwart, J. Neefjes, Drug-induced histone eviction from open chromatin contributes to the chemotherapeutic effects of doxorubicin. *Nat. Commun.* **4**, 1–13 (2013).

40. M. A. Sells, M. L. Chen, G. Acs, Production of hepatitis B virus particles in Hep G2 cells transfected with cloned hepatitis B virus DNA. *Proc. Natl. Acad. Sci.* **84**, 1005–1009 (1987).

41. L. Bai, X. Zhang, M. Kozlowski, W. Li, M. Wu, J. Liu, L. Chen, J. Zhang, Y. Huang, Z. Yuan, Extracellular Hepatitis B Virus RNAs Are Heterogeneous in Length and Circulate as Capsid-Antibody Complexes in Addition to Virions in Chronic Hepatitis B Patients. *J. Virol.* **92**, e00798-18 (2018).

42. J. Du, Y. Zhou, Q.-X. Fu, W.-L. Gong, F. Zhao, J.-C. Peng, L.-S. Zhan, Bioluminescence imaging of hepatitis B virus enhancer and promoter activities in mice. *FEBS Lett.* **582**, 3552–3556 (2008).

43. X. Chen, X. Wang, W. Liu, Y. Ren, X. Qu, J. Li, X. Yin, Y. Xu, Structures of +1 nucleosome–bound PIC-Mediator complex. *Science*. **378**, 62–68 (2022).

44. I. H. Chen, C. J. Huang, L. P. Ting, Overlapping initiator and TATA box functions in the basal core promoter of hepatitis B virus. *J. Virol.* **69**, 3647–3657 (1995).

45. T. Flecken, M.-A. Meier, P. Skewes-Cox, D. T. Barkan, M. H. Heim, S. F. Wieland, M. M. Holdorf, Mapping the Heterogeneity of Histone Modifications on Hepatitis B Virus DNA Using Liver Needle Biopsies Obtained from Chronically Infected Patients. *J. Virol.* **93** (2019), doi:10.1128/jvi.02036-18.

46. F. Alvarez-Astudillo, D. Garrido, M. Varas-Godoy, J. L. Gutiérrez, R. A. Villanueva, A. Loyola, The histone variant H3.3 regulates the transcription of the hepatitis B virus. *Ann. Hepatol.* **21**, 100261 (2021).

47. M. Locatelli, J.-P. Quivy, F. Chapus, M. Michelet, J. Fresquet, S. Maadadi, A. N. Aberkane, A. Diederichs, J. Lucifora, M. Rivoire, G. Almouzni, B. Testoni, F. Zoulim, HIRA Supports Hepatitis B Virus Minichromosome Establishment and Transcriptional Activity in Infected Hepatocytes. *Cell. Mol. Gastroenterol. Hepatol.* **14**, 527–551 (2022).

48. S. G. Lim, T. F. Baumert, C. Boni, E. Gane, M. Levrero, A. S. Lok, M. K. Maini, N. A. Terrault, F. Zoulim, The scientific basis of combination therapy for chronic hepatitis B functional cure. *Nat. Rev. Gastroenterol. Hepatol.* (2023), doi:10.1038/s41575-022-00724-5.

49. A. Osunsade, N. A. Prescott, J. M. Hebert, D. M. Ray, Y. Jmeian, I. C. Lorenz, Y. David, A Robust Method for the Purification and Characterization of Recombinant Human Histone H1 Variants. *Biochemistry*. **58**, 171–176 (2019).

50. J. T. Lis, "Fractionation of DNA Fragments by Polyethylene Glycol Induced Precipitation" in *Methods in Molecular Biology* (1980), vol. 65, pp. 347–353.

51. P. N. Dyer, R. S. Edayathumangalam, C. L. White, Y. Bao, S. Chakravarthy, U. M. Muthurajan, K. Luger, "Reconstitution of Nucleosome Core Particles from Recombinant Histones and DNA" in *Methods in Enzymology* (2003; http://www.ncbi.nlm.nih.gov/pubmed/14870657), vol. 375, pp. 23–44.

52. K. M. Krzemien, M. Beckers, S. Quack, J. Michaelis, Atomic force microscopy of chromatin arrays reveal non-monotonic salt dependence of array compaction in solution. *PLOS ONE*. **12**, e0173459 (2017).

53. N. L. Bray, H. Pimentel, P. Melsted, L. Pachter, Near-optimal probabilistic RNA-seq quantification. *Nat. Biotechnol.* **34**, 525–527 (2016).

54. M. I. Love, W. Huber, S. Anders, Moderated estimation of fold change and dispersion for RNA-seq data with DESeq2. *Genome Biol.* **15**, 550 (2014).

55. B. Langmead, S. L. Salzberg, Fast gapped-read alignment with Bowtie 2. *Nat. Methods*. **9**, 357–359 (2012).

56. A. N. Schep, J. D. Buenrostro, S. K. Denny, K. Schwartz, G. Sherlock, W. J. Greenleaf, *Genome Res.*, in press, doi:10.1101/gr.192294.115.

57. D. H. Phanstiel, A. P. Boyle, C. L. Araya, M. P. Snyder, Sushi.R: flexible, quantitative and integrative genomic visualizations for publication-quality multi-panel figures. *Bioinformatics*. **30**, 2808–2810 (2014).

58. Y. Ni, F. A. Lempp, S. Mehrle, S. Nkongolo, C. Kaufman, M. Fälth, J. Stindt, C. Königer, M. Nassal, R. Kubitz, H. Sültmann, S. Urban, Hepatitis B and D Viruses Exploit Sodium Taurocholate Co-transporting Polypeptide for Species-Specific Entry into Hepatocytes. *Gastroenterology*. **146**, 1070-1083.e6 (2014).

59. B. Qu, Y. Ni, F. A. Lempp, F. W. R. Vondran, S. Urban, T5 Exonuclease Hydrolysis of Hepatitis B Virus Replicative Intermediates Allows Reliable Quantification and Fast Drug Efficacy Testing of Covalently Closed Circular DNA by PCR. *J. Virol.* **92**, e01117-18 (2018).

Acknowledgments: The authors thank members of the David, Schwartz, and Risca labs for their support. We thank B. Y. Winer for helpful discussions and feedback. We also thank B. Wang and K. Manova-Todorova for technical assistance with atomic force microscopy. We acknowledge the use of the Integrated Genomics Operation Core and the Molecular Cytology Core Facility, supported by the NCI Cancer Center Support Grant (CCSG, P30 CA08748), Cycle for Survival, and the Marie-Josée and Henry R. Kravis Center for Molecular Oncology.

Funding:

National Institutes of Health grant T32GM115327 (NAP)

National Institutes of Health grant F99CA264420 (NAP)

National Science Foundation graduate research fellowship 2017239554 (NAP)

National Institutes of Health grant T32GM136640 (AAL)

National Institutes of Health grant F32GM140551 (AM)

Rita Allen Foundation Scholar Award (VIR)

Irma T. Hirschl/Monique Weill-Caulier Career Scientist Award (VIR)

Starr Cancer Consortium I16-0058 (VIR)

V Foundation for Cancer Research V Scholar award (VIR)

National Institutes of Health grant DP2GM150021 (VIR)

National Institutes of Health grant R01AA027327 (RES)

National Institutes of Health grant R01AI107301 (RES)

National Institutes of Health grant R01DK121072 (RES)

United States Department of Defense W81XWH-21-1-0978 (RES)

Paul G. Allen Family Foundation UWSC13448 (RES)

Irma Hirschl Trust Research Award Scholar (RES)

Josie Robertson Foundation (YD)

Pershing Square Sohn Cancer Research Alliance (YD)

MSKCC Center for Epigenetics Research (YD)

National Institutes of Health grant CCSG core grant P30CA008748 (YD)

National Institutes of Health grant SPORE P50CA192937 (YD)

National Institutes of Health grant R35GM138386 (YD)

Author contributions:

Conceptualization: NAP, RES, YD

Methodology: NAP, AM, YB

Investigation: NAP, AM, YB, AAL, CL

Visualization: NAP, AM

Funding acquisition: NAP, YD

Project administration: NAP, RES, YD

Supervision: VIR, RES, YD

Writing – original draft: NAP, YD

Writing – review & editing: NAP, AM, YB, AAL, VIR, RES, YD

Competing interests: R.E.S. is on the scientific advisory boards of Miromatrix Inc. and Lime Therapeutics and is a speaker and consultant for Alnylam Inc. All other authors declare that they have no competing interests.

Data and materials availability: MNase-seq and RNA-seq data are available at the Gene Expression Omnibus under accession numbers GSE225714, GSE225715, and GSE225716. Custom data analysis scripts are available upon request. All other data are available in the main text or the supplementary materials.

Supplementary Materials

Materials and Methods

Figs. S1 to S7

Table S1

References (*49–59*)

Data S1

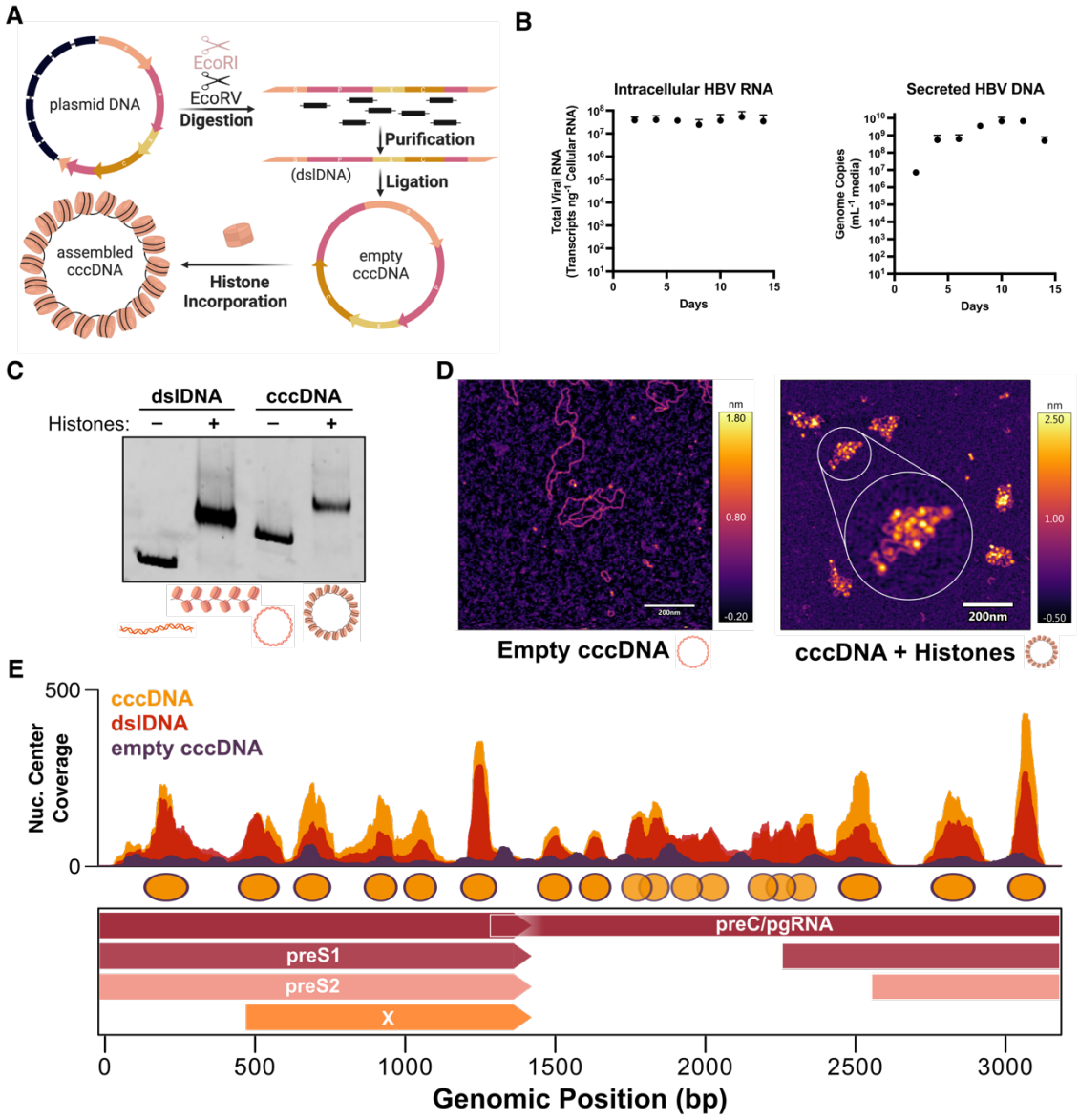

Fig. 1. Generation and validation of recombinant cccDNA minichromosomes. (**A**) Scheme illustrating minichromosome reconstitution approach. (**B**) Quantification of intracellular total HBV RNA (left) and secreted HBV DNA (right) following transfection of recombinant cccDNA into HepG2 cells. Data are means ± SD of 3 biological replicates. (**C**) Electrophoretic mobility shift of linear (dslDNA) and circular (cccDNA) HBV DNA upon incorporation of recombinant human histone octamers. (**D**) Representative atomic force micrographs of empty (left) or chromatinized (right) cccDNA minichromosomes (**E**) Coverage of centers of mononucleosome-length (120-200 bp) DNA fragments arising from digestion of chromatinized cccDNA (orange), dslDNA (red), or empty cccDNA (navy) aligned to the HBV genome and smoothed with a 50 bp window, overlaid above a schematic of the four major HBV transcripts.

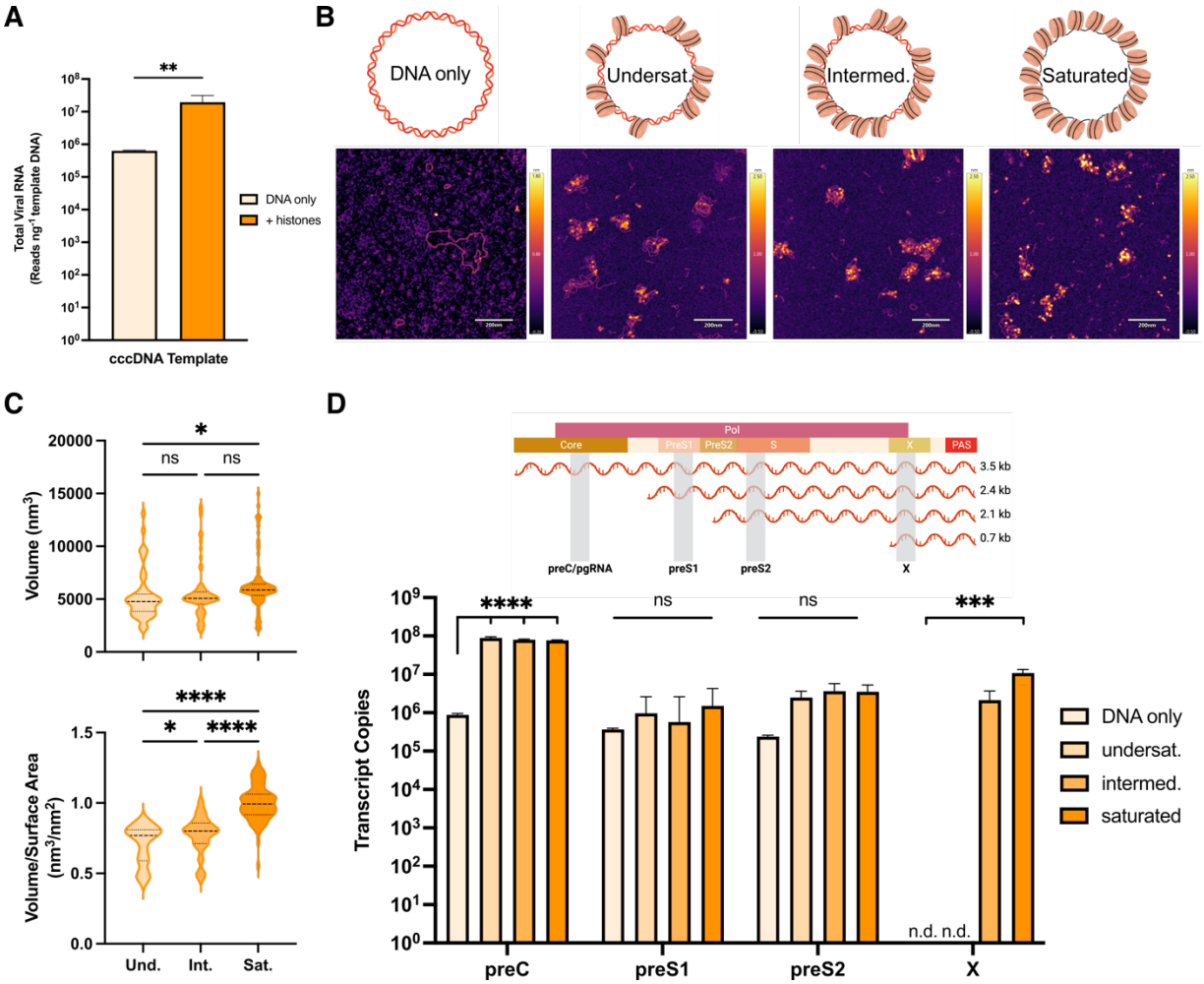

Fig. 2. Chromatin organization of reconstituted cccDNA impacts viral transcription. (**A**) Quantification of total HBV RNA produced following *in vitro* transcription (IVT) of empty or chromatinized cccDNA. (**B**) Schematics (top) and representative AFM micrographs (bottom) of differentially saturated cccDNA species. (**C**) Quantification of chromatin fiber volume (top) and compaction (bottom) for differentially saturated cccDNA species. (**D**) Quantification of transcript abundance for each major HBV transcript following *in vitro* transcription (IVT) of differentially saturated cccDNA species. Data are means ± SD and were analyzed by Welch's t-test (A) and ANOVA (C, D). *P < 0.05, **P < 0.01, ***P < 0.001, **P* <0.0001.

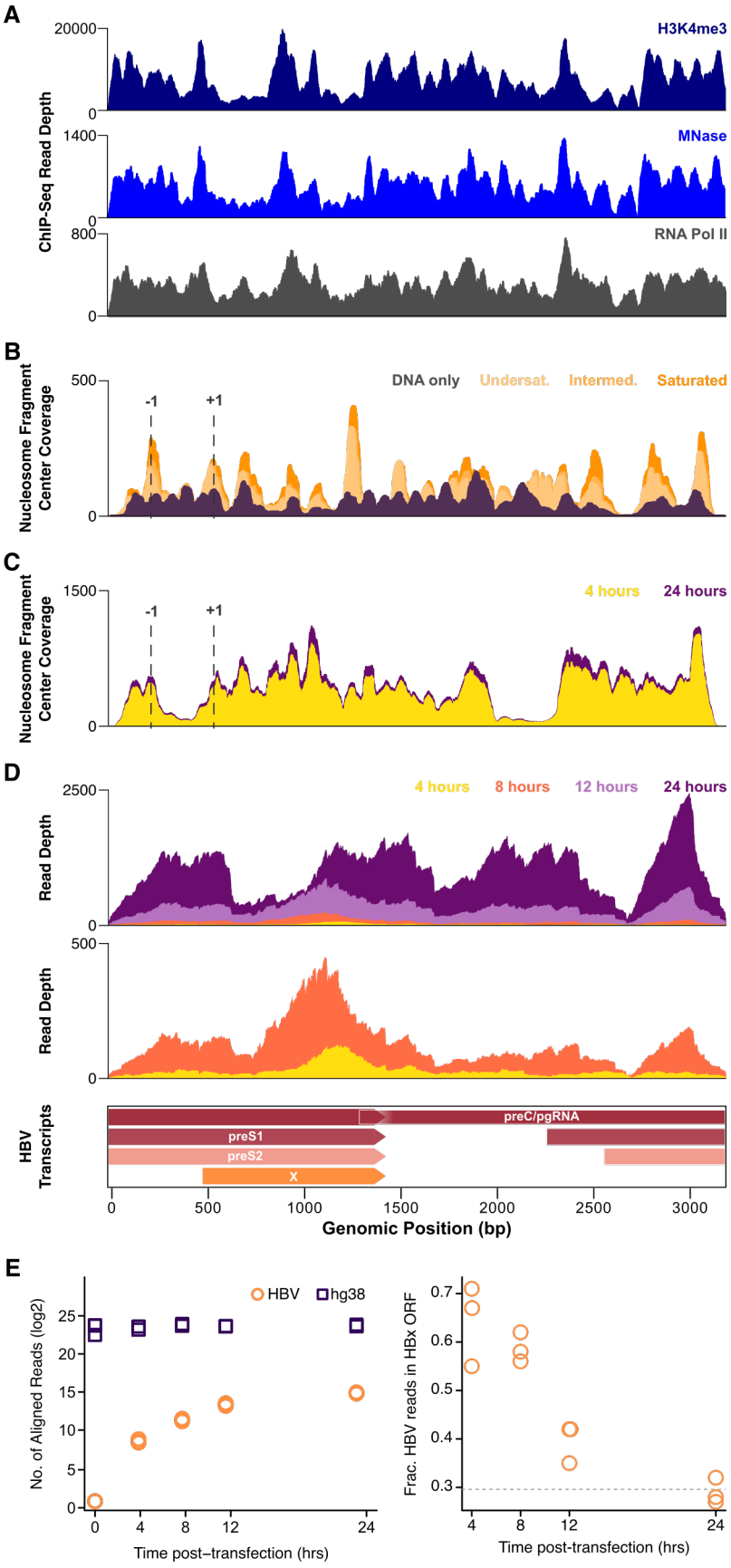
A
ChIP-Seq Read Depth
H3K4me3
MNase
RNA Pol II
B
Nucleosome Fragment Center Coverage
DNA only
Undersat.
Intermed.
Saturated
-1
+1
C
Nucleosome Fragment Center Coverage
4 hours
24 hours
D
Read Depth
4 hours
8 hours
12 hours
24 hours
HBV Transcripts
preC/pgRNA
preS1
preS2
X
Genomic Position (bp)
E
No. of Aligned Reads (log2)
HBV
hg38
Time post–transfection (hrs)
Frac. HBV reads in HBx ORF
Time post-transfection (hrs)

Fig. 3. Chromatin organization of cccDNA suggests important -1/+1 nucleosomes at the HBx TSS during early infection timepoints. (**A**) Plots of H3K4me3 (top), total sample input (middle, proxy for MNase-seq), or RNA Pol II (bottom) ChIP-seq data from primary human hepatocytes one week after infection, first reported in Tropberger et al. PNAS 2015. (**B**) 50-bp smoothed mononucleosome center coverage over the HBV genome following digestion of cccDNA chromatin arrays prepared with different levels of histone octamer saturation. (**C**) 50-bp smoothed coverage of the HBV genome by centers of unique molecular identifier (UMI)-deduplicated mononucleosome-sized fragments from *in vivo* MNase-seq 4- and 24-hours after transfection of HEK293T cells with recombinant cccDNA. (**D**) HBV genomic coordinates of RNA-seq reads mapped at all timepoints measured up to 24 hours after cccDNA transfection (top) and zoomed in on 4- and 8-hour timepoints (bottom). (**E**) Quantification of total number of aligned reads to HBV or human genomes at various RNA-seq timepoints (left) and of the fraction of HBV-aligned reads mapping to the HBx ORF (right).

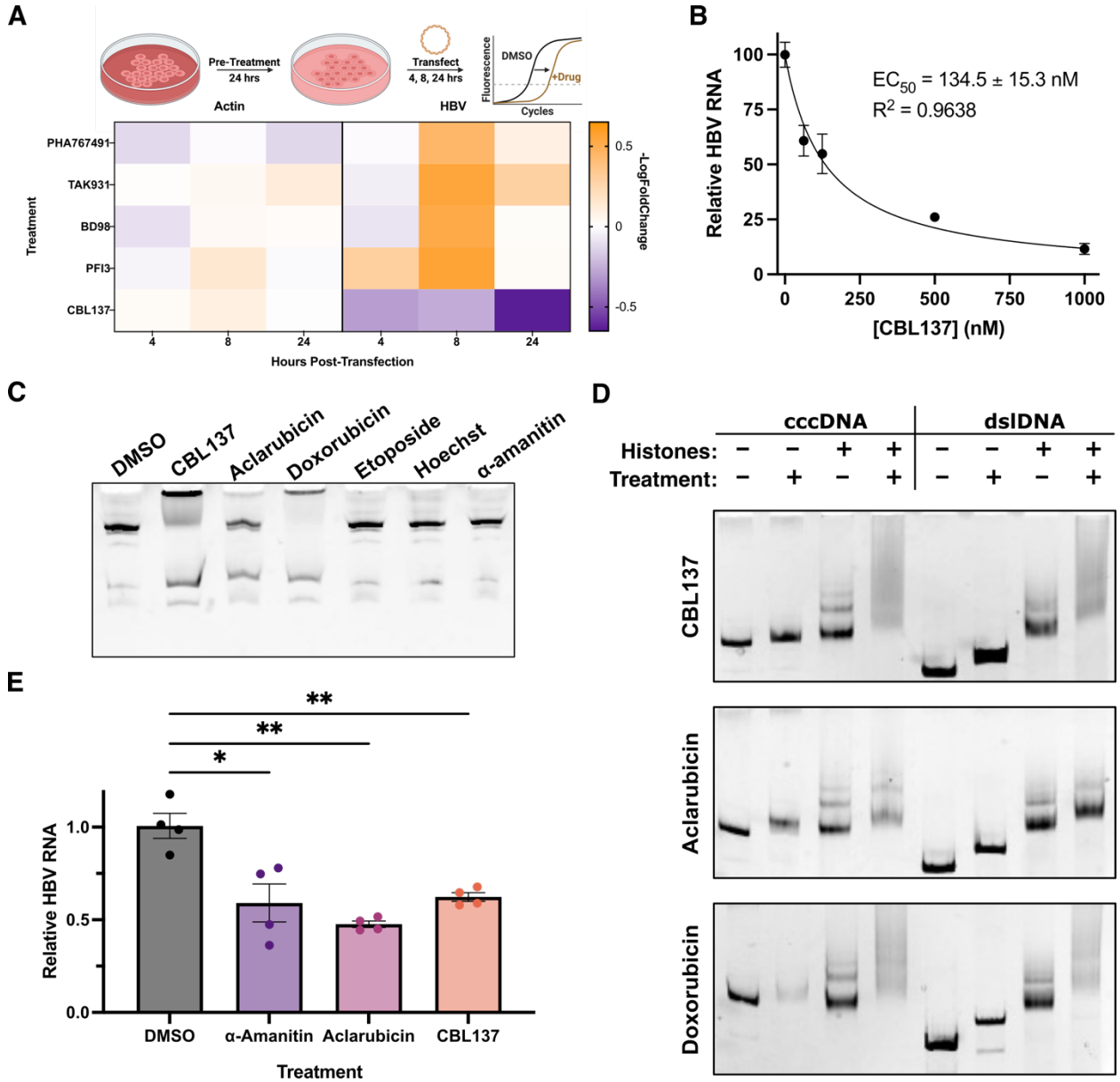

Fig. 4. Nucleosome destabilizing drugs inhibit viral transcription in cells and disrupt cccDNA integrity *in vitro*. (**A**) Heatmap depicting negative log-fold change of HBV or β-actin mRNA levels in cccDNA-transfected HEK 293T and treated with the indicated small molecule drugs. (**B**) Dose-dependence of HBV RNA levels following 24-hour treatment with the indicated CBL137 concentration. (**C**) Representative EMSA analyzing the destabilization of recombinant mononucleosomes following incubation with the indicated molecules. (**D**) Representative agarose-polyacrylamide native EMSAs of intact recombinant cccDNA and dslDNA chromatin fibers following 1-hour incubation with a 10 μM dose of the following drugs: CBL137 (top), aclarubicin(middle), and doxorubicin (bottom). (**E**) Quantification of relative HBV RNA 24-hours after transfecting HEK293T cells with recombinant cccDNA and concurrent treatment with DMSO (vehicle), 500 nM α-amanitin (Pol II poison, positive control), 125 nM CBL137, or 50 nM aclarubicin. All EMSAs are representative gels of 2 independent experiments. Data are

means ± SD and were analyzed by ANOVA (E). *P < 0.05, **P < 0.01, ***P < 0.001, **P* <0.0001.

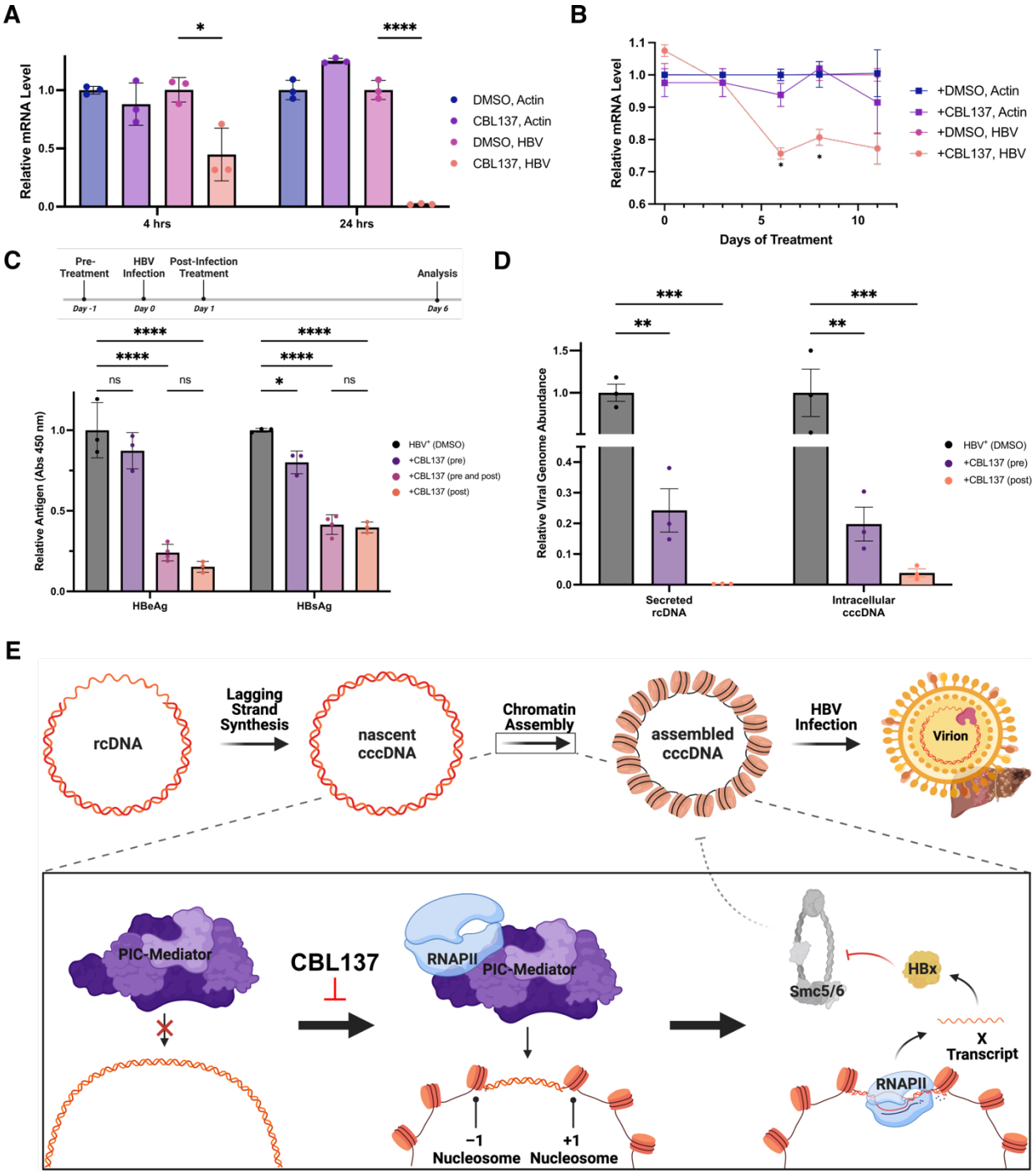

Fig. 5. CBL137 inhibits viral transcription, antigen secretion, and genome replication in hepatocyte models of HBV infection. (**A**) Quantification of relative HBV RNA after transfecting HepG2 cells with recombinant cccDNA alongside concurrent treatment with DMSO or 500 nM CBL137. (**B**) Quantification of relative HBV and β-actin RNA levels in HepG2.2.15 cells grown continuously in media containing either DMSO or 50 nM CBL137. (**C**) Quantification of HBV surface antigen (HBsAg) and secreted antigen (HBeAg) secreted from HepG2-NTCP cells following infection and 24 hr pre-incubation and/or 5 day post-infection treatment with 125 nM CBL137. (**D**) Quantification of indicated HBV genome species 6 days after infection of HepG2-NTCP cells either pre-treated with 125 nM CBL137 for 24 hrs or

cultured with the same dose for 5 days after infection. (**E**) Proposed model illustrating recognition of the HBx +1 nucleosome as a driving force behind HBV infection. Data are means ± SD and were analyzed by t-test (A, B) and ANOVA (C, D). *P < 0.05, **P < 0.01, ***P < 0.001, **P* <0.0001.

5